Designed protein pores as components for biosensors

Orit Braha[1], Barbara Walker[2], Stephen Cheley[1], John J Kasianowicz[3], Langzhou Song[4], J Eric Gouaux[4] and Hagan Bayley[1]

Background: There is a pressing need for new sensors that can detect a variety of analytes, ranging from simple ions to complex compounds and even microorganisms. The devices should offer sensitivity, speed, reversibility and selectivity. Given these criteria, protein pores, remodeled so that their transmembrane conductances are modulated by the association of specific analytes, are excellent prospects as components of biosensors.

Results: Structure-based design and a separation method that employs targeted chemical modification have been used to obtain a heteromeric form of the bacterial pore-forming protein staphylococcal α-hemolysin, in which one of the seven subunits contains a binding site for a divalent metal ion, M(II), which serves as a prototypic analyte. The single-channel current of the heteromer in planar bilayers is modulated by nanomolar Zn(II). Other M(II)s modulate the current and produce characteristic signatures. In addition, heteromers containing more than one mutant subunit exhibit distinct responses to M(II)s. Hence, a large collection of responsive pores can be generated through subunit diversity and combinatorial assembly.

Conclusions: Engineered pores have several advantages as potential sensor elements: sensitivity is in the nanomolar range; analyte binding is rapid (diffusion limited in some cases) and reversible; strictly selective binding is not required because single-channel recordings are rich in information; and for a particular analyte, the dissociation rate constant, the extent of channel block and the voltage-dependence of these parameters are distinguishing, while the frequency of partial channel block reflects the analyte concentration. A single sensor element might, therefore, be used to quantitate more than one analyte at once. The approach described here can be generalized for additional analytes.

Addresses: [1]Department of Medical Biochemistry and Genetics, Texas A&M Health Science Center, 440 Reynolds Medical Building, College Station, TX 77843-1114, USA. [2]Worcester Foundation for Biomedical Research, 222 Maple Avenue, Shrewsbury, MA 01545, USA. [3]National Institute of Science and Technology, Biotechnology Division, Building 222, Room A353, Gaithersburg, MD 20899, USA. [4]Department of Biochemistry and Molecular Biophysics, Columbia University, 650 West 168th Street, New York, NY 10032, USA.

Correspondence: Hagan Bayley
E-mail: bayley@tamu.edu

Key words: biosensor, combinatorial assembly, divalent metal cation, molecular design, single-channel current

Received: **25 April 1997**
Revisions requested: **23 May 1997**
Revisions received: **29 May 1997**
Accepted: **29 May 1997**

Chemistry & Biology July 1997, 4:497–505
http://biomednet.com/elecref/1074552100400497

Introduction

Sensors are needed for detecting a wide range of analytes. In medicine a knowledge of the concentrations of components of physiological fluids is useful in diagnosis, the levels of therapeutic agents have to be monitored and microorganisms and their toxins must be detected. In the wider environment, there is a need to quantitate levels of pollutants or to determine whether useful minerals are present. In warfare, the detection of weapons such as toxic gases is crucial, and there is considerable concern over the explosives used in terrorist attacks or present in unexploded mines. Sensors are also required in the food and beverage industries to determine the quality, and even the origin, of various products, such as coffee and wine.

Desirable features of sensors include sensitivity, speed, reversibility, a wide dynamic range and selectivity. The properties of analytes may vary enormously because they include small cations and anions, small organic molecules, macromolecules and even entire bacteria or viruses. Biosensors—sensors in which biomolecules are an integral part of the sensing element—emerge favorably when these criteria are considered [1–7].

Well-known biosensors include commercial devices for sensing glucose [3]. Recent developments include true biosensors, devices that are biomimetic, and devices that use living cells. True biosensors include those with optical detection for divalent metal cations which can be made from carbonic anhydrase [8], an enzyme in which the metal-binding site has been extensively engineered [9], and an alkaline phosphatase into which an epitope has been inserted which can be used to monitor HIV antibody levels [10]. Devices that are biomimetic include polymerized and functionalized bilayers for detecting toxins and viruses [11,12], polymer sensor arrays (loosely based on mammalian olfaction) for the electrical or optical detection of volatile organic molecules [13–15], and substrates formed by molecular imprinting, an especially promising method for the generation of new binding sites for use in sensors [16,17]. Finally, devices that use electrical or optical responses from living cells

Figure 1

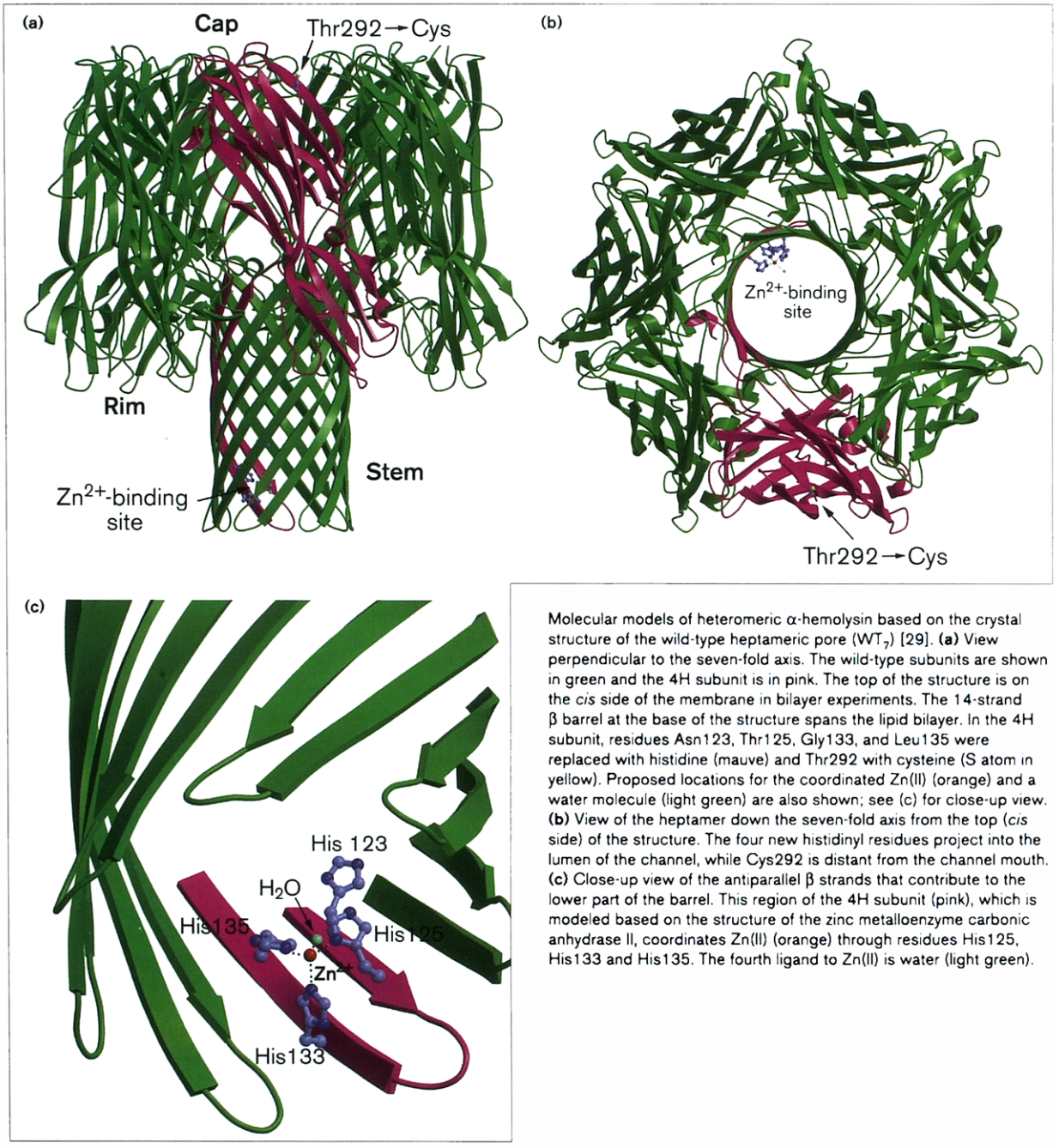

Molecular models of heteromeric α-hemolysin based on the crystal structure of the wild-type heptameric pore (WT_7) [29]. **(a)** View perpendicular to the seven-fold axis. The wild-type subunits are shown in green and the 4H subunit is in pink. The top of the structure is on the *cis* side of the membrane in bilayer experiments. The 14-strand β barrel at the base of the structure spans the lipid bilayer. In the 4H subunit, residues Asn123, Thr125, Gly133, and Leu135 were replaced with histidine (mauve) and Thr292 with cysteine (S atom in yellow). Proposed locations for the coordinated Zn(II) (orange) and a water molecule (light green) are also shown; see (c) for close-up view. **(b)** View of the heptamer down the seven-fold axis from the top (*cis* side) of the structure. The four new histidinyl residues project into the lumen of the channel, while Cys292 is distant from the channel mouth. **(c)** Close-up view of the antiparallel β strands that contribute to the lower part of the barrel. This region of the 4H subunit (pink), which is modeled based on the structure of the zinc metalloenzyme carbonic anhydrase II, coordinates Zn(II) (orange) through residues His125, His133 and His135. The fourth ligand to Zn(II) is water (light green).

containing receptors for analytes have been demonstrated [18–21].

We thought that devices incorporating protein pores as sensor elements might have advantages over existing biosensors [5]. In particular, bacterial pore-forming proteins, which are relatively robust molecules, would offer all the advantages of protein-based receptor sites together with an information-rich signal obtained by single-channel recording. Our efforts have been based on α-hemolysin (α-toxin; αHL), a 293 amino acid polypeptide secreted by *Staphylococcus aureus* as a water-soluble monomer that

assembles into lipid bilayers to form a heptameric pore [22,23]. The heptamer is remarkable for its stability in sodium dodecyl sulfate (SDS) at up to 65°C [24,25]. The biophysical properties of αHL altered in the central glycine-rich sequence, by mutagenesis or targeted chemical modification, demonstrate that this part of the molecule penetrates the lipid bilayer [26,27] and lines the lumen of the transmembrane channel [28]. As shown by X-ray crystallography, the channel through the heptamer is a 14-strand β barrel with two strands per subunit contributed by the central sequence [29].

Because of the relative simplicity of the structure of αHL and its ability to undergo self assembly, αHL is an excellent subject for investigations of membrane-protein assembly and channel function by site-directed mutagenesis and targeted chemical modification ([30,31] and references therein). It has also proved possible to design αHL polypeptides with novel properties [32], for example a light-activated pore [33]. An αHL with a binding site for a divalent metal ion, M(II), crudely designed before the structure was available, demonstrated the feasibility of metal-cation sensing with engineered pores [5,28].

One complication in previous work was that the altered pores were homomeric; that is, all seven subunits were similarly altered. A solution to this problem is presented here; in conjunction with the high resolution structure [29], the solution has allowed us to design a heteromeric pore that binds the prototypic analyte Zn(II) at a single site in the lumen of the transmembrane channel, thereby modulating the single-channel current. In addition, M(II)s other than Zn(II) modulate the current and produce characteristic signatures, and heteromers containing more than one mutant subunit exhibit distinct responses to M(II)s. An extensive collection of responsive pores suitable as components for biosensors can therefore be generated by this approach.

Results and discussion

Molecular design of heteromeric transmembrane pores

By using the three-dimensional structure of αHL [29], we designed a Zn(II)-binding subunit (4H: Asn123→His, Thr125→His, Gly133→His, Leu135→His, Thr292→Cys) in which the four histidines that were introduced by mutagenesis project into the lumen of the channel to form a cluster of imidazole sidechains (Figure 1a,b). Structural data suggest that this region of the β barrel is sufficiently flexible for at least three sidechains to act as ligands to Zn(II) in its preferred tetrahedral configuration (Figure 1c). The 4H subunit was also tagged by chemical modification of the single cysteine (at position 292) with 4-acetamido-4′-[(iodoacetyl)amino]stilbene-2,2′-disulfonate (IASD). This modification caused incremental increases in the electrophoretic mobility of heptamers in SDS-polyacrylamide gels allowing heteromers to be separated from each other and from wild-type (WT) heptamers [23]. Each disulfonate made an approximately equal contribution to the mobility, which is independent of the arrangement of the subunits about the seven-fold axis [23]. The chemical modification was distant from the channel (Figure 1); indeed, αHL(Thr292→Cys) modified with IASD, was previously shown to form fully active homomers [30].

Assembly and separation of heteromeric pores

Unlike the situation with other combinations, there is only one possible arrangement of heteromers containing six WT and one 4H subunit ($WT_6 4H_1$; Figures 1,2a). We therefore chose $WT_6 4H_1$ as the initial object for examination. The 4H mutant was prepared by *in vitro* transcription and translation (IVTT), which allowed radiolabeling with [^{35}S]methionine. WT-αHL was prepared by IVTT, when labeling was required, or purified from *Staphylococcus aureus*. WT and 4H were mixed in a molar ratio of ~5:1 and allowed to assemble on rabbit red blood cell membranes (rRBCM) or on liposomes made from egg yolk phosphatidylcholine (Figure 2b). After assembly, the 4H subunits were modified at Cys292 with IASD. The membranes were solubilized in SDS and the heteromers separated by SDS-polyacrylamide gel electrophoresis (SDS-PAGE; Figure 2c). Heptamers were eluted passively from the polyacrylamide with water, for reconstitution into bilayers for biophysical characterization. The eluted heteromers remained intact as shown by re-electrophoresis (Figure 3a), which also demonstrated that the subunits did not become scrambled; for example, WT_7 and $WT_5 4H_2$ were not formed from $WT_6 4H_1$.

In two out of five such runs, small amounts of monomer (<5%) were detected. Such breakdown is probably due to the storage conditions that the two samples experienced (e.g. for the sample displayed in Figure 3a, several freeze/thaw cycles, followed by storage at 4°C for ten days). In the other three runs, where freshly eluted heptamers were examined, monomers were not detected at all. In a definitive experiment, gel slices containing the homomers WT_7 and IASD-modified $4H_7$ were mixed and taken through the elution and storage procedures before re-electrophoresis, which again indicated no scrambling (Figure 3b). Furthermore, the eluted heptamers were free of residual proteins from the IVTT mix, as determined by silver staining (data not shown). Finally, the ratio of the subunits in each of the heteromeric forms was as expected, when determined by quantitative analysis of radiolabeled subunits from purified heteromers dissociated by heating to 95°C (Figure 3c).

Single-channel currents from the heteromer $WT_6 4H_1$

The properties of $WT_6 4H_1$ were examined by single-channel recording in a planar bilayer apparatus [34]. In this experiment, a lipid bilayer is formed across an aperture (100–200 μm diameter) in a teflon film (25 μm thick) that separates two chambers (2 ml each) containing

Figure 2

Assembly and separation of heteromeric α-hemolysin (αHL) pores. **(a)** Schematic of possible heteromer combinations resulting from the assembly of mixtures of wild-type (WT) and mutant (MUT) αHL monomers. The 20 different heteromers ($WT_{n-m}MUT_m$; n = 7, the total number of subunits; WT, open circles; mutant, filled circles) fall into $n+1$ classes categorized by the number of mutant subunits (m) in the heptamer. When mutant subunits were appropriately modified, the classes could be separated electrophoretically, see (c). The proportions of heptamers (%) in each class are shown for three starting ratios of monomers (WT:MUT, 5:1; 1:1; 1:5). The values were calculated assuming that the oligomerization process does not distinguish between WT and MUT monomers, by using $100.P_m = 100.[n!/m!(n-m)!].f_{MUT}{}^m.f_{WT}{}^{n-m}$, where: f_{MUT} and f_{WT} are the fractions of mutant and WT subunits, respectively, in the starting monomer mix. **(b)** Scheme for the assembly and separation of heteroheptameric αHL. Heteromers were formed from the desired ratio of WT and MUT subunits on either rabbit red blood cell membranes (rRBCMs) or liposomes. The heteromers were then derivatized with IASD, which introduced two negative charges for each mutant (Cys292-containing) subunit. The eight classes of heptamer, as in (a), were then separated by SDS-polyacrylamide gel electrophoresis (SDS-PAGE). The members of a particular class were obtained by elution from the polyacrylamide. **(c)** Separation of heteromers by SDS-PAGE. WT-αHL and the mutant 4H, both ^{35}S-labeled, were mixed in the ratios indicated, allowed to assemble on rRBCM and then treated as shown in (b). The membranes were solubilized in gel loading buffer containing SDS and, without heating, subjected to electrophoresis in a 7% gel. A phosphorimager display of the molecules migrating near the 200 kDa marker (myosin heavy chain) is shown. The observed ratios of oligomer classes seen in each lane approximate those calculated in (a). The left-hand lane marked 'All' contained a mixture of the solubilized samples at all five WT:4H ratios.

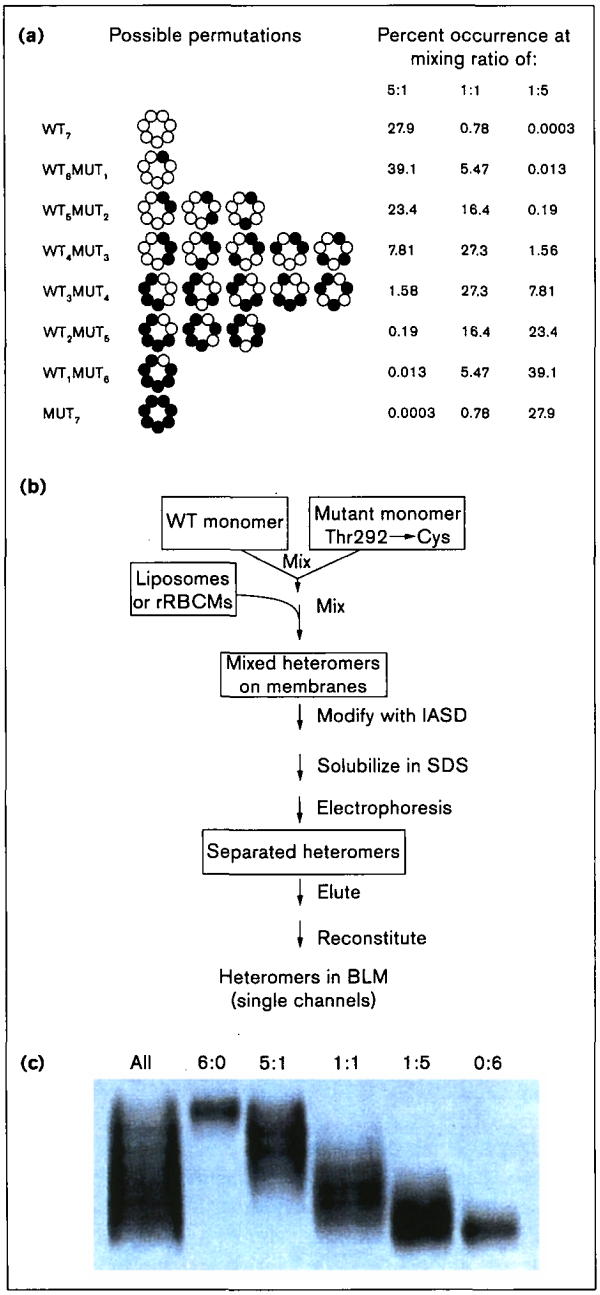

electrolyte. With a potential applied across the bilayer, the ion flux through single αHL pores can be measured with a sensitive, low-noise amplifier.

To obtain single-channel currents, the eluted heptamers, which presumably contained traces of SDS, were added at high dilution (typically 1:1000) to the *cis* chamber of the bilayer apparatus to a final concentration of 0.02–0.1 ng/ml (Figure 4). WT_64H_1 exhibited a partial and reversible channel block ($g/g_0 = 0.93 \pm 0.01$, n = 7) in the presence of 50 μM Zn(II) in the *trans* compartment with the transmembrane potential held at –40 mV (Figure 4c). WT_7 pores were not sensitive under these conditions (Figure 4b) and were unaffected by up to 500 μM Zn(II) (see also [28,35]). WT_7 is not strictly a true control for WT_64H_1. The 4H mutant was obtained from a reconstructed αHL gene (RL) in which four conservative amino acid replacements are present in the central domain (see the Materials and methods section). We therefore made WT_6RL_1 in which RL was the product of the reconstructed gene with an additional Thr292→Cys mutation, modified with IASD. This heptamer also gave no response with Zn(II) (data not shown).

Analysis of conductance histograms for WT_64H_1 obtained for a series of buffered Zn(II) concentrations (Figure 4d) yielded an EC_{50} for *trans* Zn(II) of 112 ± 23 nM (n = 3). The EC_{50} is the concentration of free M(II) that effects 50% occupancy of the binding site on 4H. Kinetic analysis of the current traces yielded a second-order association rate constant (k_{on}) for Zn(II) of $3.2 \pm 0.4 \times 10^8 M^{-1}s^{-1}$ (n = 4) which approaches the diffusion limit [36], and a dissociation rate constant (k_{off}) of $33 \pm 2 s^{-1}$ (n = 4). The EC_{50} value is lower than expected for two histidinyl ligands and approaches the values found for structures with three histidines with favorable geometry (e.g. 36 nM for a mutated retinol-binding protein [37]), suggesting that a modest distortion of the β barrel can be tolerated that places at least

Figure 3

Characterization of electrophoretically purified αHL heteroheptamers. **(a)** Heptamers were stable in SDS and the subunits did not interchange. All eight radiolabeled $WT_{n-m}4H_m$ heptamers were purified by SDS-PAGE, rerun on a 40 cm long 8% SDS-polyacrylamide gel and visualized by autoradiography. The individual heteromer species retained their relative mobilities, resulting in the staircase appearance of the image. **(b)** WT_7 and $4H_7$ did not become scrambled under the conditions used for extraction, storage and reconstitution. An excised WT_7 band was mixed and coeluted with an excised $4H_7$ band. The sample was kept at 4°C for 24 h and then stored at −20°C. The thawed sample was run on a 40 cm long 8% SDS polyacrylamide gel. The bands retained their integrity (i.e. there is no ladder of species to suggest subunit interchange). **(c)** The ratio of the WT and 4H subunits in each purified heptamer. Heptamers were made as described in (a). Half of each sample was subjected to electrophoresis without heating (top), while the other half was dissociated by heating to 95°C (bottom). The mutant monomers, modified with IASD, were separated from the more rapidly migrating WT polypeptides in a 40 cm long 10% SDS-polyacrylamide gel, allowing the quantitation of the two monomer species contained in each heptamer by phosphorimager analysis (ImageQuant, Molecular Dynamics). The expected and measured ratios are shown below each lane.

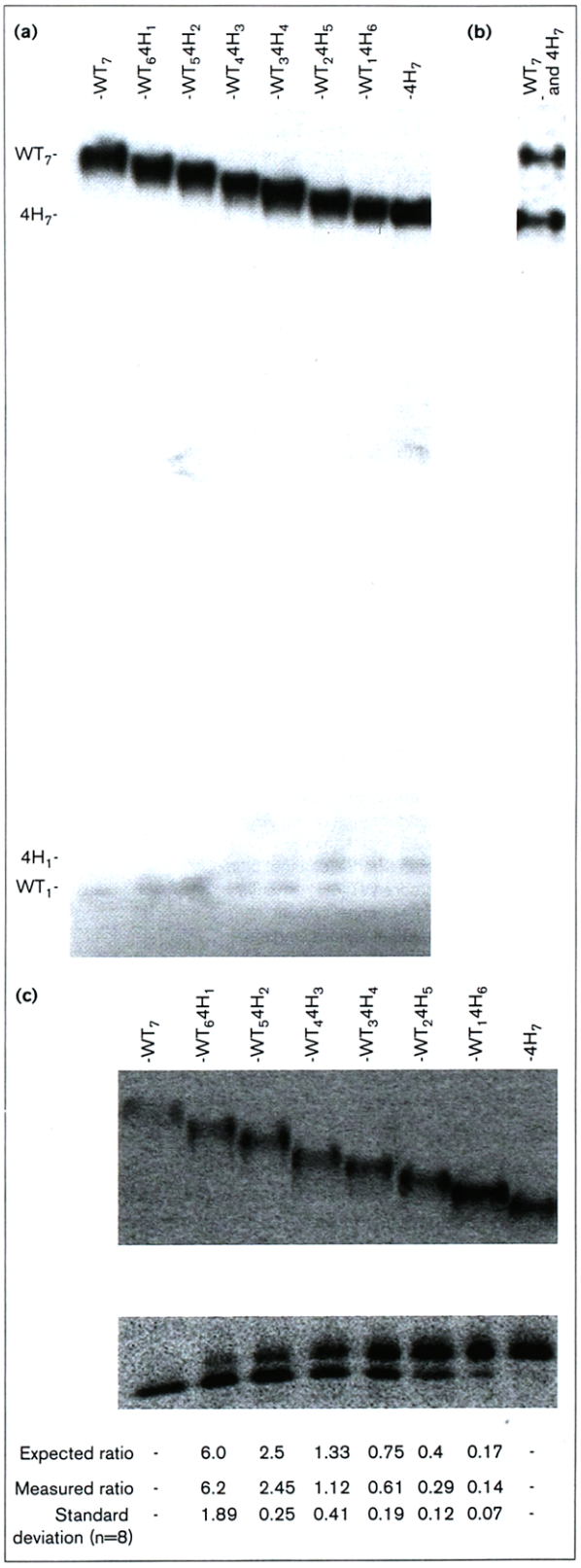

three of the four histidines in conformations suitable for coordination of the bound metal (Figure 1c). The supposed flexibility of the barrel is supported by structural data [29], the fact that for αHL in liposomes blue shifts of the fluorescent probe acrylodan, attached at single cysteine residues in the β barrel, do not alternate with residue number (as would be required for nondistorted β strands) [27] and the existence of mutants with proline residues in the central domain that form pores (B.W., unpublished observations).

The conductance of WT_7 pores (675 ± 62 pS, 1 M NaCl, 50 mM MOPS, pH 7.5, −40 mV, n = 8) is similar to that of $WT_6 4H_1$ in the absence of Zn(II) (660 ± 40 pS, n = 7). The conductance of $WT_6 4H_1$ with Zn(II) bound is reduced to 610 ± 45 pS (n = 7). At this point, various mechanisms for the partial channel block, including a simple physical blockade, distortion of the barrel, and electrostatic effects, have not been distinguished.

The heteromer $WT_6 4H_1$ shows characteristic single-channel signatures in response to various divalent metal cations

To determine whether $WT_6 4H_1$ can distinguish between different M(II)s—a requirement for a sensor element—we examined the effects of Co(II), Ni(II) and Cu(II) on single-channel currents. Each gave a characteristic signature. For example, at −40 mV 5 μM Co(II) produced bursts of noise (Figure 5a, top). At higher Co(II) concentrations (not shown), the noise was continuous and could be interpreted as the rapid interconversion of three states, one with higher conductance than $WT_6 4H_1$ in the absence of M(II). At +40 mV, two states were seen with 5 μM Co(II) (Figure 5a, bottom). The effect on current amplitude is similar to that of Zn(II) at this membrane potential, but the rates of Co(II) association and dissociation are considerably slower. These

Figure 4

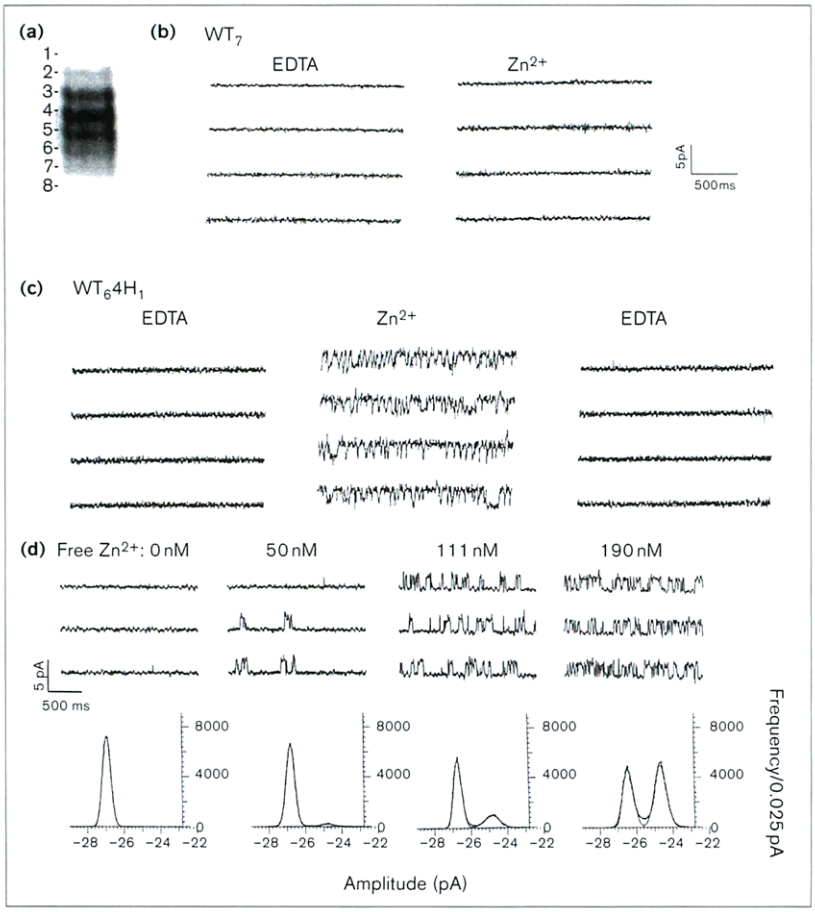

Single-channel recordings from a heteromeric αHL channel containing a Zn(II) binding site. **(a)** Autoradiogram of the SDS-PAGE separation of a ~5:1 mixture of WT and 4H, from which WT_6H_1 was eluted and used for single channel studies. Unlabeled WT was used, so the first detectable band is WT_6H_1. This band seems relatively weak here (cf. Figure 2) as it contains a single ^{35}S-labeled 4H subunit. **(b)** and **(c)** Single-channel recordings of purified WT_7 and WT_6H_1 reconstituted into planar lipid bilayers. Both *cis* and *trans* chambers contained 1 M NaCl, 50 mM MOPS, pH 7.5. Four consecutive traces of a single-channel current at −40 mV are shown for each species. (a,b) left and (b) right, currents in the presence of 100 μM EDTA; (a) right and (b) middle, currents after the addition of 150 μM $ZnSO_4$ to the *trans* side of the membrane [~50 μM free Zn(II)]. (b) WT_7, from band 1 in (a). The channel is open with an amplitude of −26.7 pA (mean = −27.0 ± 2.5 pA, n = 8). Zn(II) has no effect on the current, even when increased to 500 μM (not shown). (c) WT_6H_1, from band 2 in (a). In the presence of 100 μM EDTA the channel is open with an amplitude of −28.4 pA at −40 mV (mean = −26.3 ± 1.6 pA, n = 7). The addition of 150 μM Zn(II) to the *trans* side results in discrete fluctuations between two open states, the original state (−28.4 pA) and another of −25.7 pA (mean = −24.4 ± 1.8 pA, n = 7). The ratio of the conductance of the new state to the conductance of the original state (g/g_0) was 0.93 ± 0.01 (n = 7). **(d)** Dependence of the partial channel block of the heteromeric pore WT_6H_1 on Zn(II) concentration. Single-channel current recordings were made at various *trans* free Zn(II) concentrations with symmetrical 1 M NaCl, 50 mM MOPS, pH 7.5. Zn(II) was buffered with 100 μM pyridine-2,6-dicarboxylic acid and 10 μM EDTA. All points amplitude histograms are shown below the traces. The histograms can be fitted to the sum of two Gaussian functions, suggesting two distinct states: (i) the fully open channel, as seen in the absence of Zn(II); (ii) the partly closed, $g/g_0 = 0.93$, Zn(II)-dependent substate. The normalized areas of the Gaussian functions represent the occupancy of each state at the displayed Zn(II) concentration. When the openings or closings are short, the amplitudes of the transitions are underestimated, resulting in shifts of the peaks to lower values, for example for 190 nM Zn(II).

data also show that the responses of single-channel currents to membrane potential contain additional information about the concentration and identity of analytes.

Additional 4H heteromers exhibit different responses to divalent cations

In addition to the experiments described above, we also tested $WT_{7-n}H_n$ of all combinations. The extent of single-channel block by Zn(II) increased with the number of 4H subunits and multiple subconductance states were observed as exemplified by the data for WT_5H_2, WT_4H_3, and H_7 (Figure 5b). The specific permutations (Figure 2a) of the WT_5H_2 and WT_4H_3 pores in these recordings are not known. Single-channel recording actually provides a means to 'separate' the various permutations of each combination of heteromers. According to these data, combinatorial assembly can provide pores with characteristic responses over a wide range of analyte concentrations.

Significance

There is a need for new sensors that can detect a variety of analytes, ranging from simple ions to complex compounds and even microorganisms. Protein pores from α-hemolysin have been remodeled so that their transmembrane conductances are modulated by the association of prototype analytes—divalent metal ions, M(II)s. The lumen of the transmembrane channel can be altered to form different analyte-binding sites by design, as demonstrated here using site-directed mutagenesis, and there is the potential for new sites to be discovered by

Figure 5

Response of the heteromeric pores to different M(II)s and tuning of the sensitivity to M(II)s by adjustment of subunit composition. **(a)** Single-channel recordings from $WT_6 4H_1$ in the presence of 5 μM free Zn(II) or 5 μM free Co(II). Top, transmembrane potential −40 mV; bottom, transmembrane potential +40 mV. **(b)** The response of pores containing more than one 4H subunit to Zn(II). $WT_5 4H_2$ (concentration of free Zn(II) = 50 μM), $WT_4 4H_3$ (20 μM), and $4H_7$ (10 μM). Left, single-channel currents in the absence and presence of Zn(II). The zero current level is indicated (i = 0). Right, the corresponding all points histograms (light line, EDTA; dark line, Zn(II)).

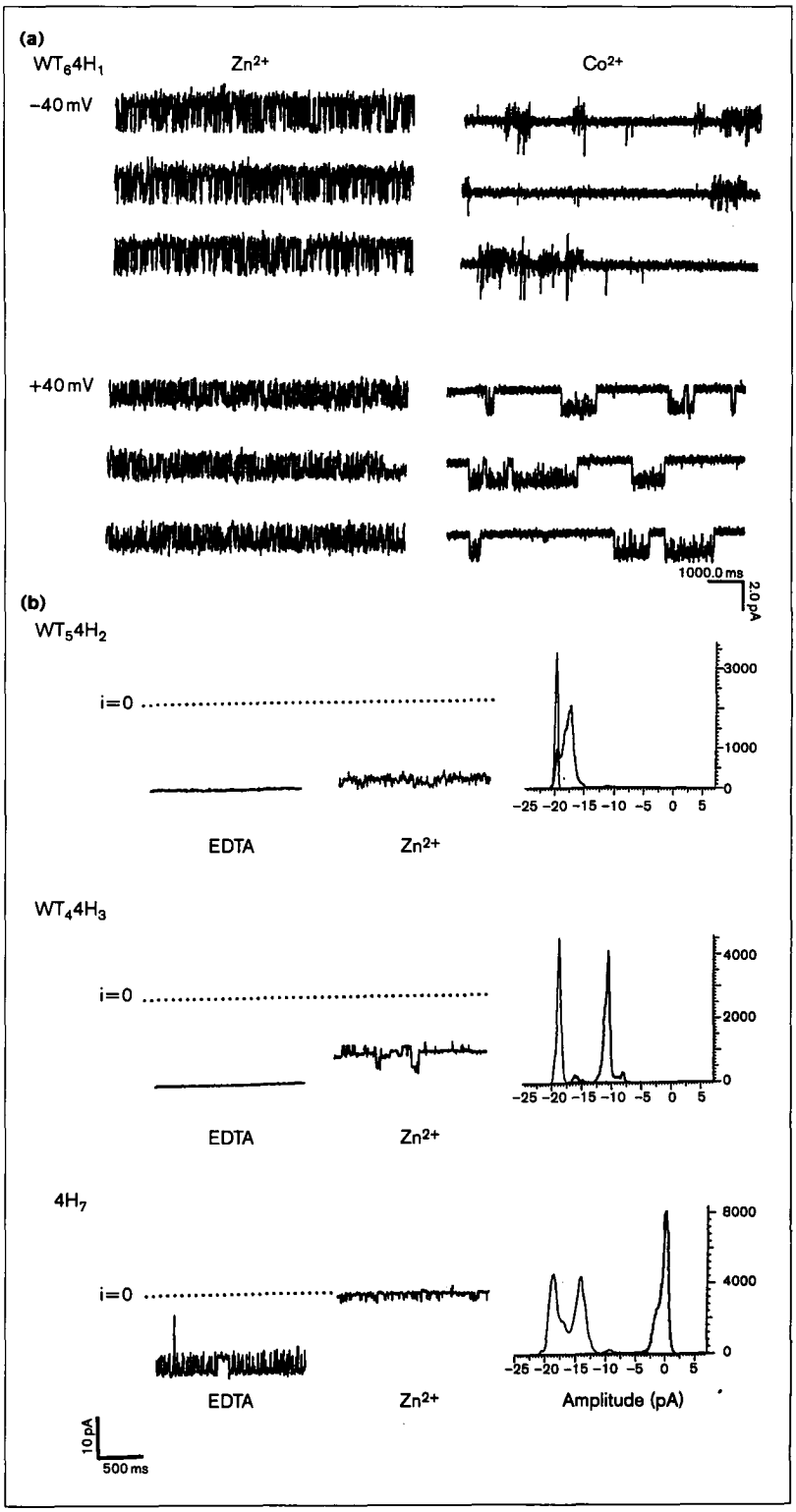

combinatorial techniques. M(II)-binding sites might also be formed by the attachment of chelating molecules by targeted chemical modification. Combinatorial assembly, again demonstrated here, is another way to generate diversity. M(II) detection is rapid, reversible and sensitive. With single-channel recording for analyte detection, the binding sites need not be fully selective because the kinetics, extent and voltage-dependence of channel block provide a distinctive analyte signature. Indeed, more than one analyte might be assayed simultaneously by this technique. The attainment of selectivity is a major problem with most sensors as they are based on an integrated signal from numerous sensor molecules.

In the future, sensor arrays with elements of overlapping analyte specificity [13–15] might be based on engineered pores to provide a yet more powerful means for the simultaneous determination of multiple analytes and to expand the dynamic range. By using the design principles illustrated here, the approach will be generalized to additional analytes by building binding sites in the lumen of the transmembrane channel or near an entrance to it. Designed pores might also have applications in other areas of biotechnology, for example for attacking cancer cells [38,39]. In basic science, they might be used to test our understanding of membrane-channel permeation, block and gating.

Materials and methods

Molecular modeling

To generate the structures in Figure 1, the coordinates of carbonic anhydrase II [40] were obtained (PDB accession number 1CA3). Two β strands (residues 91–98 and 116–121), containing the histidines that bind Zn(II), were isolated and fitted by a least squares procedure to the β strands in the stem of protomer A of the αHL structure [29]. Residues 123–126 and 132–135 of αHL were then replaced with 117–120 and 93–96 of carbonic anhydrase. The αHL sidechains were substituted back into the structure, with the exception of the histidines now at positions 123, 125, 133 and 135. The Zn(II) ion and the attached water molecule from carbonic anhydrase were left in place. In addition, Thr292 was replaced with a cysteine residue. The new molecule was drawn with Molscript [41] and a final version rendered with Raster3D [42].

Mutagenesis

The 4H mutant was made beginning with a full-length αHL gene (αHL-RL) that had been partly reconstructed with synthetic oligonucleotides to introduce unique restriction sites in the central region (residues 116–147). Full details of the reconstructed gene will be published elsewhere. Four conservative amino acid replacements are present in αHL-RL: Val124→Leu, Gly130→Ser, Asn139→Gln and Ile142→Leu. The region encoding amino acids 118–138 was removed by digestion with *Bsi*WI and *Apa*I and replaced with two synthetic duplexes (*Bsi*WI-*Spe*I and *Spe*I-*Apa*I) encoding the replacements Asn123→**His**, Val124→Leu, Thr125→**His**, Gly130→Ser, Gly133→**His**, Leu135→**His**. A 700 base pair fragment of the resulting construct, encompassing the four new histidines, was removed with *Nde*I and *Mfe*I and used to replace the corresponding sequence in αHL-Thr292→Cys [30]. The entire coding region of the resulting αHL-4H/Thr292→Cys construct was verified by sequence analysis.

Protein expression and purification

Monomeric α-hemolysin (WT-αHL) was purified from the supernatants of *S. aureus* cultures as described previously [43]. [^{35}S]Methionine-labeled WT-αHL and αHL-4H were obtained by coupled *in vitro* transcription and translation (IVTT) [43]. Separate reactions conducted with a complete amino acid premix and the premix without unlabeled methionine were mixed to yield a solution containing αHL at >10 μg/ml. In the experiments described here, αHL in the IVTT mix was partially purified by (i) treatment with 1% (w/v) polyethyleneimine (PEI) to precipitate nucleic acids, (ii) treatment with SP Sephadex C50, pH 8.0 (to remove the residual PEI), and (iii) binding to S-Sepharose Fast Flow at pH 5.2, followed by elution with 10 mM sodium acetate, pH 5.2, 500 mM NaCl. The concentration of αHL in the IVTT mix or after the purification was estimated by a quantitative hemolytic assay [43]. For 4H, it was assumed that the endpoint of the assay is the same as that of WT-αHL.

Oligomerization on red cell membranes

WT and αHL-4H were mixed in various molar ratios (6:0, 5:1, 1:1, 1:5, and 0:6) and allowed to oligomerize on rabbit erythrocyte membranes for 1 h at room temperature in 10 mM MOPS, pH 7.4, 150 mM NaCl. The membranes were washed and resuspended in 200 mM TAPS, pH 8.5, treated with 0.5 mM DTT for 5 min and then with 10 mM 4-acetamido-4′-[(iodoacetyl)amino]stilbene-2,2′-disulfonate (IASD, Molecular Probes, Eugene, OR, USA) for 1 h at room temperature to modify the Cys292 residue on the 4H polypeptide chain. The membranes were recovered by centrifugation, taken up in gel loading buffer [44], without heating, and loaded onto a 7% SDS-polyacrylamide gel (40 cm long, 1.5 mm thick) [44]. Electrophoresis was carried out for 16 h at 120 V at 4°C with 0.1 mM thioglycolate in the cathode buffer. The dried gel was subjected to phosphorimager or audioradiographic analysis.

Heteroheptamer formation and purification

Unlabeled WT-αHL and ^{35}S-labeled 4H were mixed in a 5:1 ratio (WT-αHL: 2.5 μl of 0.5 mg/ml in 20 mM sodium acetate, pH 5.2, 150 mM NaCl; ^{35}S-labeled 4H: 50 μl of 5 μg/ml). The mixed subunits were allowed to oligomerize on liposomes for 60 min at room temperature by incubation with 10 mM MOPS, pH 7.4, 150 mM NaCl (26 μl) and egg yolk phosphatidylcholine (Avanti Polar Lipids, Birmingham, AL, USA; 1.5 μl of 10 mg/ml). The latter had been bath sonicated at room temperature until clear (30 min) in 10 mM MOPS, pH 7.4, 160 mM NaCl. The mixture (80 μl) was then treated with 2 M TAPS, pH 8.5 (10 μl), and 10 mM DTT (5 μl) for 10 min at room temperature, followed by 100 mM IASD (5 μl, in water) for 60 min at room temperature. Gel loading buffer (5×, 25 μl) was then added, without heating, and a portion (50 μl) was loaded into an 8 mm wide lane of a 40 cm long, 1.5 mm thick 6% SDS-polyacrylamide gel, which was run at 4°C at 120 V for 16 h, with 0.1 mM thioglycolate in the cathode buffer. The unfixed gel was vacuum dried without heating onto Whatman 3MM chromatography paper (#3030917).

Each of the eight heptamer bands was cut from the gel, using an autoradiogram as a guide. The excised pieces were rehydrated with water (100 μl). After removal of the paper, each gel strip was thoroughly crushed in the water and the protein was allowed to elute over 16 h at 4°C. The soluble eluted protein was separated from the gel by centrifugation through a 0.2 μm cellulose acetate filter (#7016-024, Rainin, Woburn, MA, USA). A portion (20 μl) was saved for single channel studies. Sample buffer (5×, 20 μl) was added to the rest of each sample. Half was analyzed, without heating, in a 40 cm long 8% SDS-polyacrylamide gel. The other half was dissociated at 95°C for 5 min for analysis of the monomer composition in a 10% gel.

Planar bilayer recordings

A bilayer of 1,2-diphytanoyl-*sn*-glycerophosphocholine (Avanti Polar Lipids) was formed on a 100–200 μm orifice in a 25 μm thick teflon film (Goodfellow Corporation, Malvern, PA, USA) by the method of Montal and Mueller [45]. Both chambers contained 1 M NaCl, 50 mM MOPS, pH 7.5, and other solutes as described in the figure legends. 2–10 μl of the eluted protein were added to the *cis* chamber to a final concentration of 0.02–0.1 ng/ml. The bilayer was held at −40 mV with respect to the *trans* side. The solution was stirred until a channel inserted. Zn(II) was added as required, with stirring, to the *trans* chamber from a stock solution of 100 mM $ZnSO_4$ in water. Where Zn(II) was buffered, the

concentration of free Zn(II) was calculated using the program Alex [46]. Currents were recorded by using a patch clamp amplifier (Dagan 3900A with the 3910 Expander module), filtered at 5 kHz (four-pole internal Bessel filter) and stored with a digital audio tape recorder (DAS-75; Dagan Corporation, Minneapolis, MN, USA). For analysis, the data were filtered at 1–2 kHz (eight-pole Bessel filter, Model 900, Frequency Devices) and acquired at 5 kHz onto a personal computer with a Digidata 1200 D/A board (Axon Instruments) and the Fetchex program of pCLAMP 6 (Axon Instruments). The traces were filtered at 100–200 Hz for display and analysis with the Fetchan and pSTAT programs, both of pCLAMP 6. Negative current (downward deflection) represents positive charge moving from the *cis* to the *trans* chamber.

Acknowledgements

We thank Bernard Chasan for preliminary experiments, Rekha Panchal and Tom Fry for help with molecular modeling and Chris Arnoult for software. This work was supported by the ONR (H.B. and J.E.G.), DOE (H.B.), NIH (J.E.G.), NSF (J.E.G.), the Searle Scholars Program (J.E.G.) and an NAS/NRC Research Associateship (J.J.K.).

References

1. Schultz, J.S. (1991). Biosensors. *Sci. Am.* (August), 64-69.
2. Edelman, P.G. & Wang, J., eds. (1992). *Biosensors and chemical sensors: optimizing performance through polymeric materials.* American Chemical Society, Washington, DC, USA.
3. Cass, A.E.G., ed. (1992). *Biosensors: a practical approach.* IRL Press, Oxford, UK.
4. Göpel, W., Hesse, J. & Zemel, J.N., eds. (1994). *Sensors - a comprehensive survey.* VCH, Weinheim, Germany.
5. Kasianowicz, J.J., Walker, B., Krishnasastry, M. & Bayley, H. (1994). Genetically engineered pores as metal ion biosensors. *MRS Symp. Proc.* **330**, 217-223.
6. Fisher, R.J. & Fivash, M. (1994). Surface plasmon resonance based methods for measuring the kinetics and binding affinities of biomolecular interactions. *Curr. Opin. Biotechnol.* **5**, 389-395.
7. Sackmann, E. (1996). Supported membranes: scientific and practical applications. *Science* **271**, 43-48.
8. Thompson, R.B. & Jones, E.R. (1993). Enzyme-based fiber optic zinc biosensor. *Anal. Chem.* **65**, 730-734.
9. Ippolito, J.A., Baird, T.T., McGee, S.A., Christianson, D.W. & Fierke, C.A. (1995). Structure-assisted redesign of a protein-zinc binding site with femtomolar affinity. *Proc. Natl Acad. Sci. USA* **92**, 5017-5020.
10. Brennan, C.A., Christianson, K., La Fleur, M.A. & Mandecki, W. (1995). A molecular sensor system based on genetically engineered alkaline phosphatase. *Proc. Natl Acad. Sci. USA* **92**, 5783-5787.
11. Charych, D.H., Nagy, J.O., Spevak, W. & Bednarski, M.D. (1993). Direct colorimetric detection of a receptor-ligand interaction by a polymerized bilayer assembly. *Science* **261**, 585-588.
12. Charych, D., *et al.*, & Stevens, R.C. (1996). A 'litmus test' for molecular recognition using artificial membranes. *Chem. Biol.* **3**, 113-120.
13. Freund, M.S. & Lewis, N.S. (1995). A chemically diverse conducting polymer-based "electronic nose". *Proc. Natl Acad. Sci. USA* **92**, 2652-2656.
14. Lonergan, M.C., Severin, E.J., Doleman, B.J., Beaber, S.A., Grubb, R.H. & Lewis, N.S. (1996). Array-based vapor sensing using chemically sensitive, carbon black-polymer resistors. *Chem. Mater.* **8**, 2298-2312.
15. Dickinson, T.A., White, J., Kauer, J.S. & Walt, D.R. (1996). A chemical-detecting system based on a cross-reactive optical sensor array. *Nature* **382**, 687-700.
16. Mosbach, K. & Ramström, O. (1996). The emerging technique of molecular imprinting and its future impact on biotechnology. *Biotechnology* **14**, 163-170.
17. Chen, G., Guan, Z., Chen, C.-T., Fu, L., Sundresan, V. & Arnold, F.H. (1997). A glucose-sensing polymer. *Nature Biotechnol.* **15**, 354-357.
18. Tescione, L. & Belfort, G. (1993). Construction and evaluation of a metal ion biosensor. *Biotechnol. Bioeng.* **42**, 945-952.
19. Shear, J.B., Fishman, H.A., Allbritton, N.L., Garigan, D., Zare, R.N. & Scheller, R.H. (1995). Single cells as biosensors for chemical separations. *Science* **267**, 74-77.
20. Orwar, O., *et al.*, Zare, R.N. (1996). Patch-clamp detection of neurotransmitters in capillary electrophoresis. *Science* **272**, 1779-1782.
21. Graminski, G.F. & Lerner, M.R. (1994). A rapid bioassay for platelet-derived growth factor β-receptor tyrosine kinase function. *Biotechnology* **12**, 1008-1011.
22. Bhakdi, S. & Tranum-Jensen, J. (1991). Alpha-toxin of *Staphylococcus aureus. Microbiol. Rev.* **55**, 733-751.
23. Gouaux, J.E., *et al.*, & Bayley, H. (1994). Subunit stoichiometry of staphylococcal α-hemolysin in crystals and on membranes: a heptameric transmembrane pore. *Proc. Natl Acad. Sci. USA* **91**, 12828-12831.
24. McNiven, A.C., Owen, P. & Arbuthnott, J.P. (1972). Multiple forms of staphylococcal α-toxin. *J. Med. Microbiol.* **5**, 113-122.
25. Walker, B. & Bayley, H. (1995). Restoration of pore-forming activity in staphylococcal α-hemolysin by targeted chemical modification. *Protein Eng.* **8**, 491-495.
26. Ward, R.J., Palmer, M., Leonard, K. & Bhakdi, S. (1994). Identification of a putative membrane-inserted segment in the α-toxin of *Staphylococcus aureus. Biochemistry* **33**, 7477-7484.
27. Valeva, A., *et al.*, & Palmer, M. (1996). Molecular architecture of a toxin pore: a 15-residue sequence lines the transmembrane channel of staphylococcal alpha-toxin. *EMBO J.* **15**, 1857-1864.
28. Walker, B., Kasianowicz, J., Krishnasastry, M. & Bayley, H. (1994). A pore-forming protein with a metal-actuated switch. *Protein Eng.* **7**, 655-662.
29. Song, L., Hobaugh, M.R., Shustak, C., Cheley, S., Bayley, H. & Gouaux, J.E. (1996). Structure of staphylococcal α-hemolysin, a heptameric transmembrane pore. *Science* **274**, 1859-1865.
30. Walker, B. & Bayley, H. (1995). Key residues for membrane binding, oligomerization, and pore-forming activity of staphylococcal α-hemolysin identified by cysteine scanning mutagenesis and targeted chemical modification. *J. Biol. Chem.* **270**, 23065-23071.
31. Panchal, R.G. & Bayley, H. (1995). Interactions between residues in staphylococcal α-hemolysin revealed by reversion mutagenesis. *J. Biol. Chem.* **270**, 23072-23076.
32. Bayley, H. (1995). Pore-forming proteins with built-in triggers and switches. *Bioorg. Chem.* **23**, 340-345.
33. Chang, C.-Y., Niblack, B., Walker, B. & Bayley, H. (1995). A photogenerated pore-forming protein. *Chem. Biol.* **2**, 391-400.
34. Hanke, W. & Schlue, W.-R. (1993). *Planar lipid bilayers.* Academic Press, London, UK.
35. Menestrina, G. (1986). Ionic channels formed by *Staphylococcus aureus* alpha-toxin: voltage-dependent inhibition by divalent and trivalent cations. *J. Membrane Biol.* **90**, 177-190.
36. Gutfreund, H. (1995). *Kinetics for the life sciences.* Cambridge University Press, Cambridge, UK.
37. Schmidt, A.M., Müller, H.N. & Skerra, A. (1996). A Zn(II)-binding site engineered into retinol-binding protein exhibits metal-ion specificity and allows highly efficient affinity purification with a newly designed metal ligand. *Chem. Biol.* **3**, 645-653.
38. Walker, B.J. & Bayley, H. (1994). A pore-forming protein with a protease-activated trigger. *Protein Eng.* **7**, 91-97.
39. Panchal, R.G., Cusack, E., Cheley, S. & Bayley, H. (1996). Tumor protease-activated, pore-forming toxins from a combinatorial library. *Nature Biotechnol.* **14**, 852-856.
40. Eriksson, A.E., Kylsten, P.M., Jones, T.A. & Liljas, A. (1988). Crystallographic studies of inhibitor binding sites in human carbonic anhydrase II: a pentacoordinated binding of SCN^- ion to the zinc at high pH. *Proteins: Struct. Funct. Genet.* **4**, 283-293.
41. Kraulis, P.J. (1991). MOLSCRIPT: a program to produce both detailed and schematic plots of protein structure. *J. Appl. Cryst.* **24**, 946-949.
42. Merritt, E.A. & Murphy, M.E.P. (1994). Raster3D version 2.0. A program for photorealistic molecular graphics. *Acta Cryst.* **D50**, 869-873.
43. Walker, B.J., Krishnasastry, M., Zorn, L., Kasianowicz, J.J. & Bayley, H. (1992). Functional expression of the α-hemolysin of *Staphylococcus aureus* in intact *Escherichia coli* and in cell lysates. *J. Biol. Chem.* **267**, 10902-10909.
44. Laemmli, U.K. (1970). Cleavage of structural proteins during the assembly of the head of bacteriophage T4. *Nature* **227**, 680-685.
45. Montal, M. & Mueller, P. (1972). Formation of bimolecular membranes from lipid monolayers and study of their electrical properties. *Proc. Natl Acad. Sci. USA* **69**, 3561-3566.
46. Vivaudou, M., Arnoult, C. & Villaz, M. (1991). Skeletal muscle ATP-sensitive K^+ channels recorded from sarcolemmal blebs of split fibers: ATP-inhibition is reduced by magnesium and ADP. *J. Membrane Biol.* **122**, 165-175.